The Influence of Substrate Structure on Membrane Adhesion

Peter S. Swain[†,‡] and David Andelman*[,‡]

Max-Planck Institut für Kolloid- und Grenzflächenforschung, Am Mühlenberg, 14476 Golm, Germany, and School of Physics and Astronomy, Raymond and Beverly Sackler Faculty of Exact Sciences, Tel Aviv University, Ramat Aviv 69978, Tel Aviv, Israel

Received April 21, 1999. In Final Form: July 29, 1999

We consider a membrane that adheres both weakly and strongly to a geometrically structured substrate. The interaction potential is assumed to be local, via the Deryagin approximation, and harmonic. Consequently, we can analytically describe a variety of different geometries; such as, smooth substrates interrupted by an isolated cylindrical pit, a single elongated trench, or a periodic array of trenches. We present more general expressions for the adhesion energy and membrane configuration in Fourier space and find that, compared with planar surfaces, the adhesion energy decreases. We also highlight the possibility of overshoots occurring in the membrane profile and look at its degree of penetration into surface indentations.

1. Introduction

The statistical mechanics of membranes is an important branch of soft-condensed matter physics, not least because of its application to biological systems. Examples of membranes that can be studied experimentally include those of liposomes or vesicles, microemulsions, lamellar liquid crystals, as well as biological cells, such as red blood cells.[1] Of great importance is a detailed understanding of the adhesion between two membranes or between a membrane and a substrate. This adhesion occurs ubiquitously in nature, with vesicle adhesion playing a dominant role in endo- and exocytosis,[2] which is the communication of a cell with its immediate environment. Efficient drug delivery is dependent on the adhesion between a liposome and the plasma membrane of the target site,[3] while adhesion phenomena are also indispensable to biotechnology with, for example, biosensors being based on the binding of membranes to substrates.

In this paper we choose to concentrate on the latter, the adhesion between a membrane and a solid substrate, to provide theoretical support for recent experiments aimed at creating new biotechnology. All of this research has involved the study of adhesion on materials that are not flat and chemically homogeneous but that have a deliberate chemical or geometrical patterning. As far as we are aware, there has been no theoretical work describing membrane adhesion on such structured surfaces. Previous studies have looked at vesicle adhesion on simple, planar, chemically homogeneous substrates,[4,5] and we hope now to redress this imbalance.

First of all, we distinguish between weakly and strongly adhering vesicles or membranes. Weakly adhering giant vesicles have been studied using reflection interference contrast microscopy[6] and have been found to lie at distances between 300 and 400 Å from a planar substrate. Here, van der Waals attractions to the substrate are mainly counterbalanced by a repulsive entropic Helfrich force. Strongly adhering or supported membranes,[7] however, sandwich a water or polymer film between them and the substrate and typically have a much smaller separation lying at distances between 10 and 40 Å. Hydration forces are now the dominant repulsive interaction.

Supported membranes provide perhaps the most potential for biotechnological applications. They can be formed by the spreading of a bilayer over a substrate, by vesicle fusion taking place at a substrate, or by lipid monolayer transfer using a Langmuir−Blodgett technique.[7] These membranes are useful because they enable biofunctionalization of inorganic solids and provide a means to immobilize proteins (e.g., lipid coupled antigens and antibodies) with a well-defined orientation and in nondenaturing conditions.[8] The environment thus created is suitable to investigate protein−membrane coupling and protein−protein recognition processes. These processes can be used to design phantom cells that allow study of the interplay between specific (lock and key) and universal forces during cell adhesion.[7]

However, we wish to highlight the role played by supported membranes in biosensors. They can provide ultrathin, highly electrically resistant layers on top of a conducting substrate. If protein receptors are incorporated into these layers, then one can use electrical or optical means to detect or "sense" ligand binding to the receptors. Alternatively, protein ion channels can be embedded in the membrane, in which case their effect on its permeability endows the membrane with sensor-like properties.[9]

Proteins included in the membrane often have a dimension greater than its thickness (which is ∼40 Å) and so can lift the membrane off the substrate. This effect

* To whom correspondence should be addressed.
† Max-Planck Institut für Kolloid- und Grenzflächenforschung.
‡ School of Physics and Astronomy.

(1) See, for example, *Structure and Dynamics of Membranes*; Lipowsky R., Sackmann E., Eds.; Elsevier: Amsterdam, 1995.
(2) Alberts, B.; Bray, D.; Johnson, A.; Lewis, J.; Raff, M.; Roberts, K.; Walter P. *Essential Cell Biology*; Garland: New York, 1998.
(3) Lasic, D. D. In *Structure and Dynamics of Membranes*; Lipowsky, R., Sackmann E., Eds.; Elsevier: Amsterdam, 1995; pp 491−519.
(4) Seifert, U.; Lipowsky, R. *Phys. Rev. A* **1990**, *42*, 4768. Kraus, M.; Seifert, U.; Lipowsky, R. *Europhys. Lett.* **1995**, *32*, 431.
(5) Seifert, U. *Phys. Rev. Lett.* **1995**, *74*, 5060.
(6) Rädler, J. O.; Feder, T. J.; Strey, H. H.; Sackmann, E. *Phys. Rev. E* **1994**, *51*, 4526.
(7) Sackmann, E. *Science* **1996**, *271*, 43. Rädler, J.; Sackmann, E. *Curr. Opin. Solid State Material Sci.* **1997**, *2*, 330.
(8) Salafsky, J.; Groves, J. T.; Boxer, S. G. *Biochemistry* **1996**, *35*, 14773.
(9) Jenkins, A. T. A.; Bushby, R. J.; Boden, N.; Evans, S. D.; Knowles, P. F.; Liu, Q.; Miles, R. E.; Ogier, S. D. *Langmuir* **1998**, *14*, 4675.

10.1021/la990503m CCC: $18.00
Published on Web 12/03/1999

is undesirable and can be prevented by creating water pockets on the surface of the substrate that then act as protein "docking" sites. Therefore, one is naturally led to consider membrane adhesion on geometrically structured substrates that have been indented in some way. This structure can be made by a variety of methods, for example, chemical etching of silicon wafers can lead, due to their particular crystal structure, to long "V"-shaped channels.[10] Alternatively, one can use micelles made from diblock copolymers to coat any semiconductor wafer. If this is ion sputtered, then loading of the micelles in advance with an inorganic compound can provide large etching contrasts. Using this technique one can pattern a planar substrate with pits or islands on a nanometer scale.[11]

Motivated by such experiments, we discuss here a straightforward theoretical approach that allows the adhesion energy of a bound membrane to be calculated for a variety of different geometrical configurations of the substrate. The techniques used have been strongly influenced by recent work in wetting phenomena. There is now quite a substantial literature covering the effect of geometrical and chemical substrate structure on wetting films. A general form of Young's equation has been derived,[12,13] the influence of disorder[14] and corrugation[15] of the substrate on wetting transitions has been determined, and the effect of chemical patterning[16] on the shapes of adhering drop has been studied. However, we use as the inspiration for our approach a systematic description of the configuration of wetting films on nonplanar surfaces[17−19] in which one can account for the full nonlocal form of the van der Waals interaction.

There are also many interesting applications involving the adhesion of membranes on chemically structured substrates. However, we will not discuss this further here but return to it again in an accompanying publication.[20]

To start, we describe the various molecular interactions included in our model and differentiate between strong and weak adhesion. In Section 3, we consider simple, planar surfaces, that serve as the basis for nearly all the following work. The most profitable analytic approach, the Deryagin approximation, is detailed in Section 4. We consider (separately) a corrugated substrate (Section 4A) and one broken by a single (long) trench (Section 4C), a pit (Section 4D), and a periodic array of trenches (Section 4E). We calculate the equilibrium membrane profile and the adhesion energy. The variation of this energy with respect to the parameters characterizing the geometric structure is emphasized.

2. The Free Energy

To begin, we consider a membrane with an elastic modulus κ and tension σ interacting with a rough surface. For a free, almost flat membrane, which is infinite in extent, the bending energy can be described by an effective free energy functional,[21]

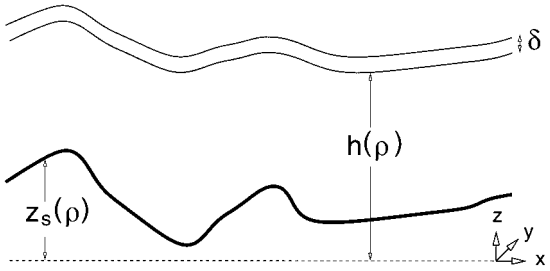

Figure 1. A membrane adhering to a rough surface. The reference $\boldsymbol{\rho}$-plane is shown as a dashed line. The height of the lower membrane lipid leaflet and the surface, measured from this plane, are denoted by $h(\boldsymbol{\rho})$ and $z_s(\boldsymbol{\rho})$, respectively. The membrane thickness is δ.

$$\int ds_1 ds_2 \sqrt{g}\left[\sigma + \frac{1}{2}\kappa(2H)^2\right] \tag{2.1}$$

where (s_1, s_2) are coordinates in the membrane surface, g is the determinant of the metric, $H = (c_1 + c_2)/2$ is the mean curvature, and c_1 and c_2 are the two principal curvatures. As the Gaussian curvature is a total divergence, the Gauss−Bonnet theorem implies that it can be ignored for a membrane with fixed topology, and we proceed to do just this here. Working in the Monge representation, let $\boldsymbol{\rho} = (x, y)$ be a two-dimensional planar vector and the heights of the surface and membrane above some reference $\boldsymbol{\rho}$-plane be $z_s(\boldsymbol{\rho})$ and $h(\boldsymbol{\rho})$, respectively. The geometry and notation used is shown in Figure 1.

For an experimental system in which giant vesicles (rather than the infinite membrane considered here) are involved, the tension usually arises due to the conservation of the vesicle total surface area. However, an additional contribution develops for a weakly adhering vesicle as the lipids making up the membrane try to move from areas far from the substrate into the more energetically favorable region near its surface. Fortunately, for our case, none of these intricacies arise, and we can consider the tension just as an external parameter.

If the membrane thickness is δ, the interaction between the surface and the membrane can be accounted for by a potential $V(h, \delta; z_s)$, and total membrane free energy is given as

$$F[h] = \int d^2\boldsymbol{\rho}\left\{\sqrt{1 + (\nabla h)^2}\left[\sigma + \frac{\kappa}{2}\left(\vec{\nabla}\cdot\frac{\vec{\nabla}h}{\sqrt{1 + (\nabla h)^2}}\right)^2\right] + V(h,\delta;z_s)\right\} \tag{2.2}$$

The interaction can be broken down into several components.[22,23] We include an external pressure, a van der Waals attraction and a repulsive force, whose nature will be different for strong and weak adhesion. In principle, other possible interactions (e.g., electrostatic forces[24]) can be added for more refined calculations. The total potential,

(10) Gerdes, S.; Ström, G. *Colloids Surf., A* **1996**, *116*, 135.
(11) Spatz, J. P.; Herzog, T.; Mössmer, S.; Ziemann, P.; Möller, M. *Adv. Mater.* **1999**, *11*, 149.
(12) Wolansky, G.; Marmur, A. *Langmuir* **1998**, *14*, 5292.
(13) Swain, P. S.; Lipowsky, R. *Langmuir* **1998**, *14*, 6772.
(14) Kardar, M.; Indekeu, J. O. *Europhys. Lett.* **1990**, *12*, 161. Li, H.; Kardar, M. *Phys. Rev. B* **1990**, *42*, 6546. Sartoni, G.; Stella, A. L.; Giugliarelli, G.; Dorsogna, M. R. *Europhys. Lett.* **1997**, *39*, 633.
(15) Parry, A. O.; Swain, P. S.; Fox, J. A. *J. Phys.: Condens. Matter* **1996**, *8*, L659. Swain, P. S.; Parry, A. O. *Eur. Phys. J. B* **1998**, *4*, 459.
(16) Gau, H.; Herminghaus, S.; Lenz, P.; Lipowsky, R. *Science* **1999**, *283*, 46.
(17) Andelman, D.; Joanny, J. F.; Robbins, M. O. *Europhys. Lett.* **1988**, *7*, 731. Robbins M. O.; Andelman, D.; Joanny, J. F. *Phys. Rev. A* **1991**, *43*, 4344.
(18) Netz, R. R.; Andelman, D. *Phys. Rev. E* **1997**, *55*, 687.
(19) Harden, J. L.; Andelman, D. *Langmuir* **1992**, *8*, 2547.
(20) Swain, P. S.; Andelman, D., to be published.
(21) Canham P. B. *J. Theor. Biol.* **1970**, *26*, 61. Helfrich, W. *Z. Naturforsch., C* **1973**, *28*, 693.
(22) Lipowsky, R. In *Structure and Dynamics of Membranes*; Lipowsky, R., Sackmann, E., Eds.; Elsevier: Amsterdam, 1995; pp 521−602.
(23) Israelachvili, J. N. *Intermolecular and Surface Forces*; Academic: London, 1992.
(24) For a treatment of the adhesion of charged membranes at flat surfaces, see Nardi, J.; Feder, T.; Bruinsma, R.; Sackmann E. *Europhys. Lett.* **1997**, *37*, 371. Nardi, J.; Bruinsma, R.; Sackmann E. *Phys. Rev. E* **1998**, *58*, 6340.

used in eq 2.2, is then

$$V(h,\delta;z_s) = p(h - z_s) + V_{vdw}(h,\delta;z_s) + V_{rep}(h;z_s) \tag{2.3}$$

A different dependence on the surface height has been emphasized as, in general, the interaction potential is a *functional* of z_s. Note that in eq 2.2, the potential V is integrated over the *projected area*, $A_0 = \int d^2\boldsymbol{\rho}$, only because all nonlocal effects of the solid roughness and membrane fluctuations are, in principle, incorporated into the potential itself.

The existence of an external pressure p in eq 2.3 implies that there is a difference in pressure across the membrane. Recalling that the membrane is infinite in its lateral extent, the pressure couples linearly to the membrane height and could arise, for example, from the existence of macromolecules on one side of the membrane only.[25]

The van der Waals attraction that the membrane feels toward the solid surface is given by

$$V_{vdw}(h,\delta;z_s) = -[W(h;z_s) - W(h+\delta;z_s)] \tag{2.4}$$

where $W(h;z_s)$ is an interfacial-like van der Waals potential. Equation 2.4 arises because of the bilayer nature of the membrane and can be understood as a supposition of two wetting layers. One of these has height $h + \delta$, whereas the other is of height h and has a Hamaker constant of opposite sign. For a wetting fluid film of thickness $h(\boldsymbol{\rho})$ resting on a solid substrate, with a rough surface configuration given by $z = z_s(\boldsymbol{\rho})$, $W(h; z_s)$ satisfies the following:[17]

$$W(h;z_s) = \int_{h(\boldsymbol{\rho})}^{\infty} dz \int d^2\boldsymbol{\rho}' \int_{-\infty}^{z_s(\boldsymbol{\rho}+\boldsymbol{\rho}')} dz'\, w(\boldsymbol{\rho}', z-z') \tag{2.5}$$

In eq 2.5, the kernel interaction is

$$w(\mathbf{r}) = \frac{A}{\pi^2}\left(\frac{1}{r}\right)^{2m+2} \tag{2.6}$$

Following convention, we have denoted the Hamaker constant A and will usually set the integer $m = 2$ to model nonretarded van der Waals interactions. Equation 2.5 comes from the sum over all possible pair interactions between the molecules making up two half spaces that are capped by either the surface $z = h(\boldsymbol{\rho})$ or $z = z_s(\boldsymbol{\rho})$.

Notice that eq 2.5 is a function of $h(\boldsymbol{\rho})$ but a functional of $z_s(\boldsymbol{\rho})$. For a flat membrane on top of a smooth and planar solid surface, which will be discussed in the following section, this functional dependence on $z_s(\boldsymbol{\rho})$ can be ignored and then (for $m = 2$)

$$W(h,z_s) = \frac{A}{12\pi}\frac{1}{(h - z_s)^2} \tag{2.7}$$

This is the standard result for the van der Waals potential between two semi-infinite bodies with planar surfaces held a distance $h - z_s$ apart.[23]

To counterbalance this attractive force, a repulsive interaction is included, and we define two different possible scenarios; they are, the weak and strong adhesion regimes.

A. Weakly Adhering Membranes. In this case, we consider a repulsive force that is entropic in origin. This force arises because of the surface cutting off the region that can be sampled by the membrane as it undergoes thermal fluctuations. A renormalization group description is the only general approach that can be used to describe such effects but, depending on the nature of the intermolecular interactions, a simple supposition ansatz can sometimes suffice.[22] Helfrich[26] was the first to include an entropic term in the potential but considered only tensionless membranes. When a membrane is under tension, the extent to which it can fluctuate is much reduced and there is a corresponding decrease in the entropic repulsion. Although there is some controversy of the exact form of the potential,[22,27,28] a decay exponential in h has been verified by Monte Carlo simulation.[29] Unfortunately, analytical expressions are only available for the tension- and rigidity dominated regimes. However, a simple argument by Seifert[5] gives a form that takes the correct limit for $\sigma \to 0$ or $h \to 0$ and has the dominant h exponential decay in the tension regime. For simplicity, we choose

$$V_{fluc}(h) = \frac{6T^2}{(2\pi)^2\kappa}\left(\frac{\Omega}{\sinh \Omega h}\right)^2 \tag{2.8}$$

where

$$\Omega = \left(\frac{\pi\sigma}{2T}\right)^{1/2} \tag{2.9}$$

We denote the temperature by T and have set here and hereafter the Boltzmann constant k_B to unity. The prefactor of eq 2.8 has been chosen to be consistent with the renormalization group description[22] as $h \to \infty$, but we note that the exact value has no special importance in our model. In the limit of zero tension, eq 2.8 tends to the well-known result $3T^2/(2\pi^2\kappa h^2)$. For large Ωh, the potential decays exponentially as $\exp(-2\Omega h)$.

Equation 2.8 was initially assumed to be valid only for a membrane fluctuating near a flat surface. However, a number of different methods have shown that the Helfrich term can also be used for a rough substrate if h is replaced by the local height of the membrane. This approach has been adopted by several authors considering spatially inhomogeneous scenarios[30−32] and agrees with scaling arguments based on exact solutions.[33] Consequently, for a rough surface, we choose a fluctuation repulsion satisfying $V_{fluc}(h; z_s) = V_{fluc}(h - z_s)$, with $V_{fluc}(h)$ given by eq 2.8.[34]

B. Strongly Adhering Membranes. Because the membrane now lies much closer to the substrate (a typical distance can be 30 Å as compared with 340 Å for the weakly adhering case), the repulsive interaction becomes dominated by hydration forces. Although their exact origin is not entirely understood (see ref 23), experimentally they decay exponentially[35] and have an angstrom range

$$V_{hyd}(h) = b\sigma\, e^{-\alpha h} \tag{2.10}$$

where b is a dimensionless number and α an inverse

(25) An additional contribution arises due to the finite membrane thickness, but as we assume that this is fixed throughout the membrane, it is just a constant that we neglect.

(26) Helfrich, W. Z. *Naturforsch.* **1978**, *33*, 305.
(27) Helfrich, W.; Servuss, R. M. *Il Nuovo Cimento D* **1984**, *3*, 137.
(28) Evans, E. *Langmuir* **1991**, *7*, 1900.
(29) Netz, R. R.; Lipowsky, R. *Europhys. Lett.* **1995**, *29*, 345.
(30) Bruinsma, R.; Goulian, M.; Pincus, P. *Biophys. J.* **1994**, *67*, 746.
(31) Bar-Ziv, R.; Menes, R.; Moses, E.; Safran, S. A. *Phys. Rev. Lett.* **1995**, *75*, 3356.
(32) Menes, R.; Safran S. A. *Phys. Rev. E* **1997**, *56*, 1891.
(33) Netz, R. R. *J. Phys. (France) I* **1997**, *7*, 833.
(34) As δ is constant, we can ignore its influence on the fluctuation interaction; it is only the lower lipid leaflet that defines the volume between the membrane and the substrate and so determines V_{fluc}.
(35) Gawrisch K., Ruston D., Zimmerberg J., Parsegian V. A., Rand R. P. and Fuller N. *Biophys. J.* **1992**, *61*, 1213.

length, typically $\alpha^{-1} \simeq 2-3$ Å. For a rough substrate we again assume that we can replace h by the relative height and so use the local expression for the interaction potential, $V_{hyd}(h - z_s)$, in the free energy. Such an assumption seems reasonable because of the very short-range nature of the interaction in eq 2.10.

C. The Adhesion Energy. To summarize, the total free energy consists of

$$F[h] = \int d^2\boldsymbol{\rho}\left\{\sqrt{g}\left[\sigma + \frac{1}{2}\kappa(2H)^2\right] + p(h - z_s) + V_{vdw}(h,\delta;z_s) + V_{rep}(h - z_s)\right\} \quad (2.11)$$

that is, a bending energy made up of tension (coupled to the membrane area) and rigidity (coupled to its total mean curvature squared, H^2) terms and an interaction potential V given by eq 2.3. The latter contains a contribution from an external pressure, the full nonlocal van der Waals interaction, and a local repulsion, V_{rep}, which we consider either as a fluctuation (see eq 2.8) or a hydration interaction (as in eq 2.10).

One of the most relevant quantities in experiments is the membrane adhesion energy. Within our general mean-field approach, the optimal height of the membrane is that which minimizes eq 2.11. The value of the free energy of the system when the membrane takes up this optimum configuration, F_{min}, leads to the following natural definition of the adhesion energy per unit area

$$U \equiv -\left(\frac{F_{min}}{A_0} - \sigma\right) \quad (2.12)$$

Here, A_0 is the total area of the *projected* reference $\boldsymbol{\rho}$-plane, $A_0 = \int d^2\boldsymbol{\rho}$.

Notice that in eq 2.12, a tension-dependent term has been added. Doing so conveniently shifts the origin in such a way that the adhesion energy for a completely flat membrane has no tension-dependent contribution. This result agrees with one's intuitive picture and is necessary because the membrane tension couples to the entire membrane area and not just to any excess area arising from a nonplanar configuration. Consequently, for a membrane adhering to a flat wall and being itself flat [$h(\boldsymbol{\rho}) = h_0$ for some constant h_0], the adhesion energy is simply given as the negative of the interaction potential experienced by the membrane. For example, from eq 2.11 (see also eq 2.2)

$$F_{min} = A_0[\sigma + V(h_0,\delta;0)] \quad (2.13)$$

and therefore eq 2.12 implies that

$$U = -V(h_0,\delta;0) \quad (2.14)$$

and the tension contribution vanishes. Hence, U is positive for all sufficiently attractive potentials, V.

D. Rescaling of Lengths and Interactions. Before we proceed and calculate the adhesion energy U for different types of corrugated and rough surfaces, it proves profitable to extract two natural lengthscales present in the problem.

The first of these is provided by the ratio between the Hamaker constant, A, appearing in the van der Waals potential (eq 2.5), and the tension σ,[36]

$$a = \left(\frac{A}{2\pi\sigma}\right)^{1/2} \quad (2.15)$$

whereas the second describes the crossover between the tension and the rigidity dominated regimes

$$\xi = (\kappa/\sigma)^{1/2} \quad (2.16)$$

Using these definitions, eqs 2.2 and 2.5 become, respectively,

$$\frac{1}{\sigma}F[h] = \int d^2\boldsymbol{\rho}\left\{\sqrt{1 + (\nabla h)^2}\left[1 + \frac{1}{2}\xi^2\left(\vec{\nabla}\cdot\frac{\vec{\nabla}h}{\sqrt{1 + (\nabla h)^2}}\right)^2\right] + \frac{1}{\sigma}V(h,\delta;z_s)\right\} \quad (2.17)$$

and

$$\frac{1}{\sigma}W(h;z_s) = \frac{2a^2}{\pi}\int_{h(\rho)}^{\infty} dz \int d^2\boldsymbol{\rho}' \int_{-\infty}^{z_s(\rho+\rho')} dz'[\rho'^2 + (z - z')^2]^{-(m+1)} \quad (2.18)$$

In the next sections, eq 2.17 will be minimized and the adhesion energy U will be calculated for various corrugated and rough surfaces. However, first we discuss the case of a simple, flat surface.

3. A Planar Surface: Choice of Physical Parameters

For a planar and homogeneous solid surface, mean-field theory predicts that the membrane also adopts a flat configuration,

$$h(\boldsymbol{\rho}) = h_0 \quad (3.1)$$

where we use the subscript zero to denote all planar quantities. Here, we set $z_s(\boldsymbol{\rho}) = 0$ to ensure a zero average surface height. The van der Waals term (for $m = 2$) also simplifies considerably

$$\frac{1}{\sigma}V_{vdw}(h, \delta; 0) = -\frac{a^2}{6}\left(\frac{1}{h^2} - \frac{1}{(h + \delta)^2}\right) \quad (3.2)$$

and the repulsion satisfies eqs 2.8 and 2.10 for weak and strong adhesion, respectively.

The membrane height h_0 obeys $V'(h_0) = \partial V/\partial h = 0$ (balance of forces), whereas the adhesion energy, eq 2.12 is

$$-\frac{U_0}{\sigma} \equiv \frac{V_0(h_0, \delta)}{\sigma} = \begin{cases} \dfrac{p}{\sigma}h_0 - \dfrac{a^2}{6}\left[\dfrac{1}{h_0^2} - \dfrac{1}{(h_0 + \delta)^2}\right] + \dfrac{3T}{4\pi\kappa}\sinh^{-2}(\Omega h_0) & \text{weak adhesion} \\ \dfrac{p}{\sigma}h_0 - \dfrac{a^2}{6}\left[\dfrac{1}{h_0^2} - \dfrac{1}{(h_0 + \delta)^2}\right] + b\, e^{-\alpha h_0} & \text{strong adhesion} \end{cases} \quad (3.3)$$

where $V_0(h, \delta) \equiv V(h, \delta; 0)$. Equation 3.3 is useful because it serves as the starting point for which all our perturbation theories provide corrections.

(36) de Gennes, P. G. *Rev. Mod. Phys.* **1985**, *57*, 827.

Table 1. Numerical Values of Model Parameters

general parameters			
$\kappa = 35T$	$\sigma = 1.7 \times 10^{-5}$ Jm^{-2}	$\delta = 38$ Å	$p = 0$
$\Omega \simeq 8.07 \times 10^{7}$ m^{-1}	$b \simeq 5.47 \times 10^{4}$	$\alpha^{-1} = 2.2$ Å	$T = 4.1 \times 10^{-21}$ J
weak adhesion			
$A = 8.67 \times 10^{-22}$ J	$a \simeq 28.5$ Å	$h_0 \simeq 11.85a \simeq 338$ Å	$U_0 \simeq 1.1 \times 10^{-4}\,\sigma$
$\xi \simeq 32.25a$	$v \simeq 8.04 \times 10^{-6}a^{-2}\sigma$	$\xi_\sigma \simeq 352.62a$	$\xi_\kappa \simeq 106.64a$
$\chi \simeq 0.302$	$\eta_+ \simeq 0.0309a^{-1}$	$\eta_- \simeq 0.0028a^{-1}$	$L \simeq 259.1a$
strong adhesion (supported membrane)			
$A = 2.6 \times 10^{-21}$ J	$a \simeq 49.3$ Å	$h_0 \simeq 0.61a \simeq 30$ Å	$U_0 \simeq 0.298\sigma$
$\xi \simeq 18.62a$	$v \simeq 22.85a^{-2}\sigma$	$\xi_\sigma \simeq 0.21a$	$\xi_\kappa \simeq 1.97a$
$\chi \simeq 9.44$	$\eta_+ \simeq (0.359 + 0.357i)a^{-1}$	$\eta_- \simeq (0.359 - 0.357i)a^{-1}$	$L \simeq 22.3a$

At this point, to facilitate comparison with experimental systems, we discuss the numerical values of our model parameters. A particular example is detailed in Table 1, where $T = 4.1 \times 10^{-21}$ J at room temperature and k_B was set to unity. For simplicity, the external pressure is set equal to zero throughout

$$p = 0 \tag{3.4}$$

Let us discuss now the choice of parameters for weak and strong adhering membranes, separately. (i) For weak adhesion, an effective value of the Hamaker constant is used ($A = 8.67 \times 10^{-22}$ J $\simeq 0.21\ T$). This value is quite small to approximately model the screening effect of ions in the solution surrounding the membrane.[23] Setting $\sigma = 1.7 \times 10^{-5}$ Jm^{-2}, the rescaling length, a, is $\simeq$28.5 Å, and h_0 is calculated to be $\simeq 11.85a$ or $\simeq$338 Å, which is in agreement with experimental results.[6] Such a value is reassuring because the expression in eq 3.2 for the van der Waals interaction is only valid for $h < 500$ Å before retardation effects begin to become important.[37] From Figure 2, one can see that $V_0(h_0, \delta) \simeq -1.1 \times 10^{-4}\sigma$ and so the adhesion energy is positive as expected:

$$U_0 \equiv -V_0(h_0,\delta) \simeq 1.1 \times 10^{-4}\sigma = 1.87 \times 10^{-9}\ \text{J m}^{-2} \tag{3.5}$$

(ii) If we now turn to strong adhesion, ion effects can be ignored, and we use a larger value of the Hamaker constant ($A = 2.6 \times 10^{-21}$ Jm$^{-2} \simeq 0.63\ T$).[6] This approach implies that $a \simeq 49.3$ Å and $h_0 \simeq 0.61a \simeq 30$ Å, which are values that are in agreement with those measured using specular reflection of neutrons.[38] The various parameters specifying the hydration force (see eq 2.10) are

$$b = (0.93\ \text{J m}^{-2})/\sigma \simeq 5.47 \times 10^{4} \qquad \alpha^{-1} = 2.2\ \text{Å} \tag{3.6}$$

which are values that are in accordance with those measured by Gawrisch et al.[35] This time (see Figure 2), $V_0(h_0, \delta) \simeq -0.298\sigma$ and, therefore,

$$U_0 \simeq 0.298\sigma = 5.07 \times 10^{-6}\ \text{J m}^{-2} \tag{3.7}$$

which is significantly greater than the result in eq 3.5.

Throughout the paper, we will keep to the particular values of the membrane and external parameters specified here and in Table 1. It is sometimes convenient to express lengths in terms of the length a and energies (per unit area) in terms of the tension σ, which is arbitrarily taken to have the same numerical value for weakly and strongly adhering membranes. We should say, however, that our model can offer only qualitative, or at best semiquantitative comparison with experiment.

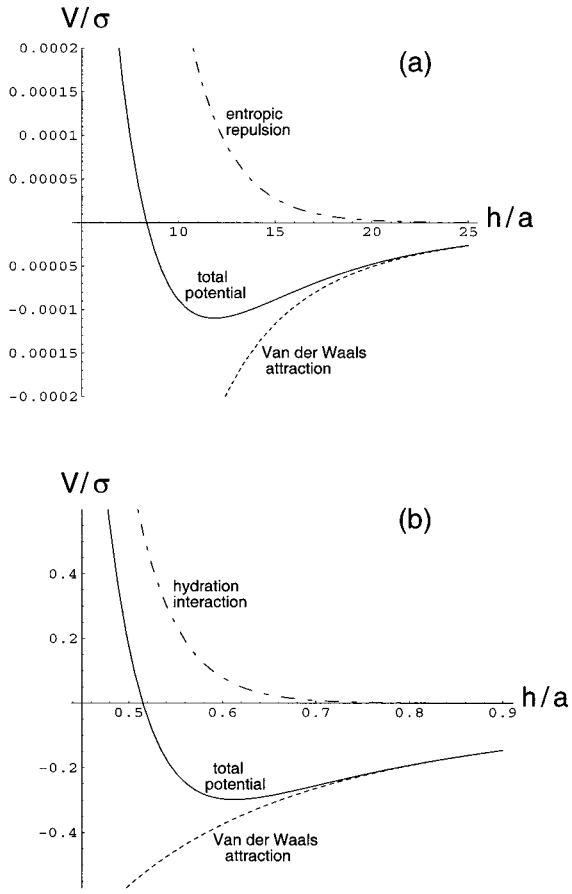

Figure 2. A plot of the various interactions described in Section 2, with parameter values given in Table 1, for a membrane (a) weakly and (b) strongly adhering to a planar substrate. All potentials are measured in units of the tension, $\sigma = 1.7 \times 10^{-5}$ Jm^{-2}, and lengths in terms of a. The system can be seen to equilibrate at $h_0 \simeq 12a$ and $h_0 \simeq 0.6a$ for weak and strong adhesion, respectively.

4. The Deryagin Approximation

One of the most useful approaches, which provides good opportunity for analytic progress, is the Deryagin approximation.[39] First of all, the full nonlocal van der Waals potential (eqs 2.4 and 2.5), is replaced by a planar potential that is simply a function of the local relative height coordinate. Because the pressure term is always local and V_{rep} already has this form, the total potential is written as

(37) Lipowsky, R.; Leibler, S. *Phys. Rev. Lett.* **1986**, *56*, 2541.
(38) Johnson, S. J.; Bayerl, T. M.; McDermott, D. C.; Adam, G. W.; Rennie, A. R.; Thomas, R. K.; Sackmann, E. *Biophys. J.* **1991**, *59*, 289.
(39) Deryagin, B. V. *Kolloidn. Zh.* **1955**, *17*, 827. Deryagin, B. V.; Churaev, N. V.; Muller V. M. *Surface Forces*; Consultants Bureau: New York, 1987.

$$V(h,\delta;z_s) \simeq V_0(h-z_s,\delta) = p(h - z_s) + V_{vdw}(h-z_s,\delta;0) + V_{rep}(h - z_s) \quad (4.1)$$

where $V_0(h,\delta) = V(h,\delta;0)$ as before. Notice that eq 4.1 corresponds to replacing $z_s(\boldsymbol{\rho} + \boldsymbol{\rho}')$ in eq 2.5 with $z_s(\boldsymbol{\rho})$; that is, removing the functional dependence of the potential on z_s. The resulting free energy is then expanded to second-order in $h - h_0$ and z_s. Because the equilibrium position of the membrane is given by setting the variation to zero, the first-order term in h and z_s vanishes, yielding

$$\frac{1}{\sigma}F[h] \simeq \int d^2\boldsymbol{\rho}\left\{1 + \frac{1}{2}(\nabla h)^2 + \frac{1}{2}\xi^2(\nabla^2 h)^2 + \frac{1}{\sigma}V_0(h_0,\delta) + \frac{v}{2\sigma}(h - h_0 - z_s)^2\right\} \quad (4.2)$$

with

$$v = \frac{\partial^2}{\partial h^2}V(h,\delta;0)|_{h=h_0} = -a^2\sigma\left[\frac{1}{h_0^4} - \frac{1}{(h_0 + \delta)^4}\right] + V''_{rep}(h_0) \quad (4.3)$$

Writing $\delta h(\boldsymbol{\rho}) = h(\boldsymbol{\rho}) - h_0$, the Euler−Lagrange equation, giving the value of δh which minimizes eq 4.2, is relatively straightforward:

$$(\kappa\nabla^4 - \sigma\nabla^2 + v)\delta h(\boldsymbol{\rho}) = v z_s(\boldsymbol{\rho}) \quad (4.4)$$

To solve eq 4.4, it is convenient to convert to Fourier space. Defining for any function $f(\boldsymbol{\rho})$

$$\tilde{f}(\mathbf{q}) = \int d^2\boldsymbol{\rho}\, f(\boldsymbol{\rho})e^{-i\mathbf{q}\cdot\boldsymbol{\rho}} \quad (4.5)$$

we find

$$\delta\tilde{h}(\mathbf{q}) = \frac{\tilde{z}_s(\mathbf{q})}{1 + q^2\xi_\sigma^2 + q^4\xi_\kappa^4} \quad (4.6)$$

with the correlation lengths having the usual definitions:[22]

$$\xi_\sigma^2 = \sigma/v \qquad \xi_\kappa^4 = \kappa/v \quad (4.7)$$

For small $q\xi_\sigma$, eq 4.6, implies that the membrane follows the rough surface. However, as $q\xi_\sigma$ increases, both the tension and the rigidity act to dampen this effect.

Using eqs 2.12, 4.2, and 4.6, one can write the adhesion energy as

$$\frac{U}{\sigma} = 1 - \frac{1}{A_0}\int d^2\boldsymbol{\rho}\left\{1 + \frac{V_0(h_0,\delta)}{\sigma}\right\} - \frac{v}{A_0\sigma}\int\frac{d^2\mathbf{q}}{2(2\pi)^2}\left\{\frac{q^2\xi_\sigma^2 + q^4\xi_\kappa^4}{1 + q^2\xi_\sigma^2 + q^4\xi_\kappa^4}\right\}|\tilde{z}_s(\mathbf{q})|^2 \quad (4.8)$$

By defining the excess in the adhesion energy to be with respect to the planar case [recall that $U_0 = -V_0(h_0, \delta)$] as

$$\Delta U \equiv U - U_0 = U + V_0(h_0,\delta) \quad (4.9)$$

we obtain

$$\frac{\Delta U}{\sigma} = -\frac{1}{A_0}\int\frac{d^2\mathbf{q}}{2(2\pi\xi_\sigma)^2}\left\{\frac{q^2\xi_\sigma^2 + q^4\xi_\kappa^2}{1 + q^2\xi_\sigma^2 + q^4\xi_\kappa^4}\right\}|\tilde{z}_s(\mathbf{q})|^2 \quad (4.10)$$

which is only strictly valid up to $O(q^4)$ because higher order terms in q have not been included in our starting equation.

Equation 4.10 has buried within it several assumptions that we will now make more explicit. It is important to realize that eq 4.6 is not necessarily the general solution to eq 4.4 but just a particular solution. The general solution itself can be found by adding eq 4.6 to the homogeneous solution; that is, the solution of eq 4.4 when z_s is set to zero. This solution then contains the four constants of integration required to satisfy any boundary conditions. Therefore, eq 4.10 is only correct when the homogeneous solution of eq 4.4 is identically zero, which is true, for example, at a sinusoidally corrugated substrate (see Section 4A). Otherwise, although eq 4.10 is certainly included in U, it is not the whole picture and, in this case, it may well be better to work entirely in real space.

For the particular experimental system specified in Section 3, one can calculate the various correlation lengths. These lengths have been included in Table 1 for completeness.

The approximations used in this section have, as their basis, essentially a perturbation theory (assuming $h - h_0 - z_s$ is small) around the planar value of the adhesion energy, U_0. Generally, one can only believe such an approach if the correction term, ΔU, is much smaller than the result upon which it is trying to improve. Consequently, our findings are strictly only valid when

$$\left|\frac{\Delta U}{U_0}\right| \ll 1 \quad (4.11)$$

which in fact limits the roughness of the substrates we can consider.

A. Sinusoidally Corrugated Surface. The simplest case to look at is a sinusoidally corrugated surface

$$z_s(\boldsymbol{\rho}) = c\sin(qx) \quad (4.12)$$

with an amplitude c and period $2\pi/q$. Solving eq 4.4, one can show that

$$\delta h(\boldsymbol{\rho}) = \frac{c\sin(qx)}{1 + q^2\xi_\sigma^2 + q^4\xi_\kappa^4} \quad (4.13)$$

Similarly, ΔU in eq 4.10 is

$$\frac{\Delta U}{\sigma} = -\frac{c^2}{4\xi_\sigma^2}\left(\frac{q^2\xi_\sigma^2 + q^4\xi_\kappa^4}{1 + q^2\xi_\sigma^2 + q^4\xi_\kappa^4}\right) \quad (4.14)$$

which is valid for small cq.

In Figure 3, U/U_0 (using the parameters of Table 1) is plotted as a function of the rescaled wavenumber aq for both weak and strong adhesion. From eq 4.13, the average height of the membrane is unchanged from the planar result h_0. However, as q increases and the surface becomes corrugated with shorter wavelengths, the adhesion energy decreases (relative to the planar case).

Two factors contribute to this result. First, there is an extra bending energy cost as the membrane tries to follow the substrate configurations. Second, the roughness acts, despite the increased surface area, to reduce the absolute

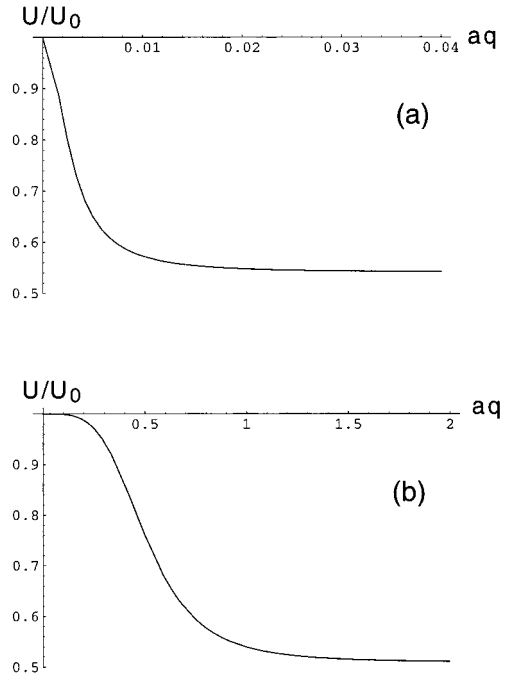

Figure 3. A plot of the adhesion energy versus the rescaled wavenumber aq of a sinusoidally corrugated surface. For (a) weak adhesion, the surface amplitude is set to $c = 5a \simeq 143$ Å, whereas for (b) a strongly adhering membrane, it is set much smaller at $c = 0.16a \simeq 8$ Å. All other parameters are given in Table 1. For these values of c, U soon reaches a small (<1) asymptotic value, which implies that our perturbation theory remains valid for all q.

value of the membrane potential energy. This reduction occurs because of the nonlinear way z_s enters eq 2.5, and is best seen in eq 4.2. Given that we are approximating the total potential harmonically and so as a parabola, eq 4.2 shows that the effect of the surface structure is to lift (v is always positive) the membrane potential out from the minimum, V_0. An identical, more familiar, phenomenon takes place when one wishes to include Gaussian thermal fluctuations in a mean-field Hamiltonian. Both contributions to the free energy are thus made more positive and so the adhesion energy (see eq 2.12) is decreased.

For large q, U flattens out; any point on the membrane is almost equidistant from a crest or trough on the substrate surface and so there is little energetic benefit in mimicking them. From eq 4.14 we have the following[40] in the limit $q \gg \max(\xi_\sigma^{-1}, \xi_\kappa^{-1})$

$$\Delta U \simeq -\frac{c^2\sigma}{4\xi_\sigma^2} \tag{4.15}$$

which is in accordance with $U/U_0 \simeq 0.54$ and $U/U_0 \simeq 0.51$ (see Figure 3) for weak and strong adhesion, respectively. For small $q \ll \min(\xi_\sigma^{-1}, \xi_\kappa^{-1})$, the membrane can always follow these long wavelength perturbations,

$$\Delta U \simeq -\frac{\sigma c^2 q^2}{4} \tag{4.16}$$

and U remains q dependent.

It is worth pointing out the very different x-axis scales and choices of c in Figure 3. For weak adhesion where $c = 5a$ (i.e., $c \simeq 143$ Å), the adhesion energy "bottoms out"

(40) Assuming eq 4.11 is still valid.

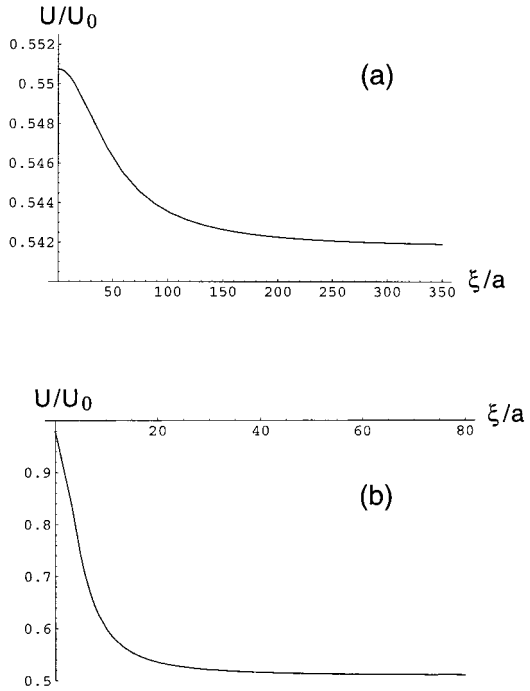

Figure 4. The adhesion energy for a (a) weakly and (b) strongly adhering membrane above a corrugated surface, with $c = 5a \simeq 143$ Å and $q = 0.02/a$ for the former and $c = 0.16a \simeq 8$ Å and $q = 1/a$ for the latter. Increasing ξ/a corresponds to increasing κ/A. All other parameter values are given in Table 1.

for $q \simeq 0.03/a$. For strong adhesion, c is much smaller ($c \simeq 8$ Å), and much larger values of q are needed before the structure of the substrate is effectively smeared away. The values of c in both cases were chosen to ensure that eq 4.11 remains valid and one can see that U/U_0 is never much smaller than 0.5. Our perturbation theory appears to work for amplitudes c that which do not grow significantly bigger than approximately one third of the height taken by the membrane above a planar substrate (i.e., $h_0/3$).

By noting that $\xi_\kappa^2 = \xi\xi_\sigma$, eq 4.14 can be written as

$$\frac{\Delta U}{\sigma} = -\frac{c^2}{4}\left(\frac{q^2}{\dfrac{1}{1+q^2\xi^2} + q^2\xi_\sigma^2}\right) \tag{4.17}$$

and so one can also look at the effect of the elastic modulus κ on the adhesion energy by plotting U/U_0 against the crossover length ξ/a while keeping ξ_σ constant (see Figure 4). As ξ increases, κ becomes greater than the Hamaker constant, A. This increased bending energy (coupled with the fact that the membrane average position is fixed at h_0) leads to a raise in magnitude of ΔU, and so the adhesion energy decreases relative to U_0.

B. Membrane Profiles for Piecewise Constant Surfaces. For piecewise constant surfaces, eq 4.4, is quite easily solved (see Appendix A). For substrates with one-dimensional symmetry, $z_s(\boldsymbol{\rho}) = z_s(x)$, the general solution is (for constants c_0, c_1, c_2, and c_3)

$$\delta h(x) = c_0 e^{\eta_+ x} + c_1 e^{-\eta_+ x} + c_2 e^{\eta_- x} + c_3 e^{-\eta_- x} + z_s \tag{4.18}$$

where the expressions for $\eta_\pm$ are given in eq A3 in Appendix A. The implications of eq 4.18 will be explored in the following subsections.

C. An Isolated Trench. We next consider a single, infinitely long trench parallel to the y axis and of width

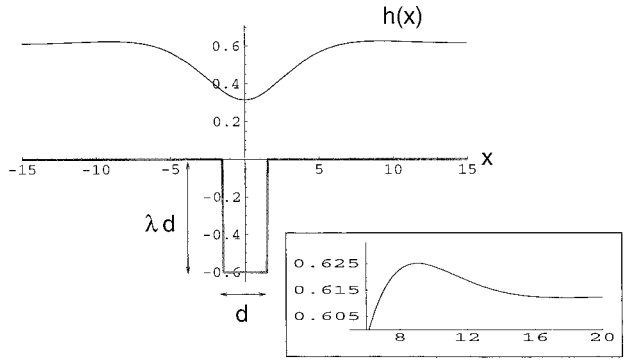

Figure 5. The membrane profile $h(x)$ for strong adhesion to a solid surface (thick line) broken by a single trench of width $d = 3a \simeq 148$ Å and depth λd, with $\lambda = 0.2$. The inset region shows a blowup of the profile, with scales chosen to emphasize the overshoot. The local adhesion energy is $U/U_0 \simeq 0.51$. All lengths are in units of a without explicit statements for clarity. Parameter values are given in Table 1 (strong adhesion) and only the lower lipid leaflet is shown.

d and depth λd. The height profile of the surface takes either of two fixed values: $-\lambda d$ for $|x| < d/2$, and zero otherwise (see Figure 5). This profile can be also written as

$$z_s(\boldsymbol{\rho}) = z_s(x) = -\lambda d\{\theta(x + d/2) - \theta(x - d/2)\} \qquad (4.19)$$

where $\theta(x)$ is the Heaviside step function, being only nonzero (and equal to unity) for positive x. The one-dimensional solution of eq A1 is given by eq 4.18, with z_s taking either of the fixed values $-\lambda d$ for $|x| < d/2$ or zero otherwise. The constants of integration can be determined from the following boundary conditions

$$\delta h(-x) = \delta h(x) \qquad (4.20)$$

$$\delta h(\pm x) \to 0 \qquad \text{as } |x| \to \infty \qquad (4.21)$$

and by imposing continuity (up to the third derivative in x) at the edges of the trench, $x = \pm d/2$. The final solution is (for positive $x \geq 0$)

$$\frac{1}{\lambda d}\delta h(x) = \begin{cases} -1 + \frac{1}{2}k_- e^{-\eta_+ d/2}\cosh(\eta_+ x) + \frac{1}{2}k_+ e^{-\eta_- d/2}\cosh(\eta_- x) & \text{for } 0 \leq x \leq d/2 \\ -\frac{1}{2}k_-\sinh\left(\frac{\eta_+ d}{2}\right)e^{-\eta_+ x} - \frac{1}{2}k_+\sinh\left(\frac{\eta_- d}{2}\right)e^{-\eta_- x} & \text{for } x \leq d/2 \end{cases} \qquad (4.22)$$

and

$$k_\pm = 1 \pm \frac{1}{\sqrt{1 - 4\chi^4}} \qquad (4.23)$$

Here, $\chi = \xi/\xi_\kappa$ (see eq A4).

In Figure 5, the membrane profile is sketched for a supported membrane (strong adhesion case) with the same parameters as those given in Table 1. The trench is specified by $d = 3a$ (i.e., 148 Å) and $\lambda = 0.2$. The membrane can be seen to follow the contour of the surface, as expected from the general prediction (eq 4.6), without developing a similar discontinuity to that occurring at the boundary

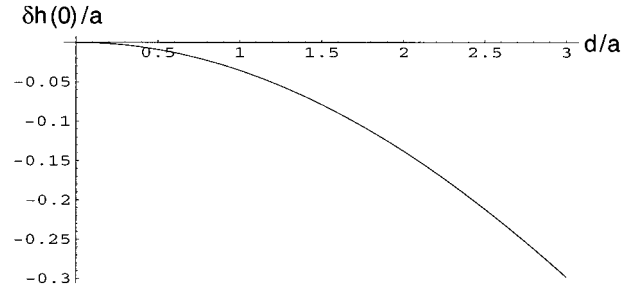

Figure 6. The height of the membrane $\delta h(0) = h(0) - h_0$ at the center of an isolated trench of width d and depth λd, where $\lambda = 0.2$. See Table 1 (strong adhesion) for choices of the other parameters.

of the trench. In addition, it can be seen that an overshoot is present, with the membrane having a height greater than h_0 (for an extensive discussion of overshoots see ref 32). From eq 4.22, $\delta h = h - h_0$ can be shown to be negative for all $x > d/2$, providing $\eta_\pm$ are real. Therefore, the overshoot can only arise if $\eta_\pm$ go complex. A necessary condition found from eq A3 is that $1 - 4\chi^4 < 0$ or that

$$2\xi > \xi_\sigma \qquad (4.24)$$

i.e., one must be in the rigidity dominated regime ($4\kappa > \sigma^2/v$).

Equation 4.24 can be understood by realizing that the rigidity term in the free energy (eq 4.2) prevents the membrane from turning any sharp corners (see Appendix B). For a pure interface ($\kappa = 0$ and $\sigma \neq 0$), eq 4.24 cannot be satisfied and, within the Deryagin approximation, no overshoot ever occurs.

It is also interesting to look at the extent to which the membrane penetrates into the trench. A natural measure of this quantity is the membrane height in the trench center:

$$\delta h(0) = \lambda d\left(-1 + \frac{1}{2}k_- e^{-\eta_+ d} + \frac{1}{2}k_+ e^{-\eta_- d}\right) \qquad (4.25)$$

In Figure 6, this quantity is plotted against d/a, the trench width (here, λ simply scales out; see eq 4.25). For larger d, the membrane is able to enter the trench more easily because there is less bending energy cost in the smoother configuration required to do so. For small d/a, $\delta h(0) \to 0$ and $h(0)$ tends towards the planar value of the average membrane height as the trench becomes increasingly more narrow. In the opposite limit (not yet visible in Figure 6), where $d/a \gg 1$, eq 4.25 implies that $\delta h(0)/a \to -\lambda d/a$, although here we are pushing our perturbation theory beyond its region of validity.

The adhesion energy (eq 2.12) is defined as an energy per unit of projected area. To obtain a finite contribution in the case of an isolated surface perturbation like a trench, we need to consider one occurring in an otherwise flat surface of *finite* lateral extent L. Hence, using a local definition, involving a cutoff L, we can write that the change in U, ΔU (up to second-order in δh), is

$$\Delta U = -\frac{1}{2L}\int_0^L dx\{\sigma(\delta h')^2 + \kappa(\delta h'')^2 + v(\delta h - z_s)^2\} \qquad (4.26)$$

From eq 4.18 we can see that for real η, the cutoff should be proportional to η_+^{-1} because of the exponential decay. However, for $\chi > 1/\sqrt{2}$, both η_+ and η_- are no longer real and it is straightforward to show that

$$\eta_+ = \eta_-^* = \frac{1}{2}\xi^{-1}\left\{\sqrt{2\chi^2+1} + i\sqrt{2\chi^2-1}\right\} \quad (4.27)$$

where the asterisk denotes complex conjugation. In this case, eq 4.18 implies that for $x > d/2$, the profile has an exponential term, $\exp(-x\sqrt{2\chi^2+1}/2\xi)$, and so a natural choice for L is

$$L = 8 \times \max\left(\frac{d}{2}, \frac{1}{Re\{\eta_+\}}\right) \quad (4.28)$$

where the prefactor was chosen by examining some numerical solutions for the profile. If η_+ is complex, then eq 4.27 implies that $1/Re\{\eta_+\} = 2\xi/\sqrt{2\chi^2+1}$. Using this definition, $L \simeq 22.3a$ for the system specified in Table 1, which is a sensible value (see Figure 5).

Using eqs 4.22 and 4.26, one can show that

$$\frac{\Delta U}{\sigma} = -\frac{\lambda^2 d}{32L}\left\{\left(\frac{k_-}{\Lambda_+}\right)^2 I(\Lambda_+,\Lambda_+) + \left(\frac{k_+}{\Lambda_-}\right)^2 I(\Lambda_-,\Lambda_-) + \left(\frac{2\xi}{d}\right)^2 k_+k_- I(\Lambda_+,\Lambda_-)\right\} \quad (4.29)$$

where $\Lambda_\pm \equiv \eta_\pm d$ is introduced,

$$I(u,v) = uv(u+v)(e^u-1)(e^v-1)\, e^{-(u+v)(1/2+L/d)} \times \left[\frac{e^{(u+v)(L/d-1/2)}}{w(u,v)} - \frac{1}{2}\right] \quad (4.30)$$

with

$$w(u,v) = 1 - \frac{u(e^v-1)+v(e^u-1)}{ue^u(e^v-1)+ve^v(e^u-1)}$$

and $k_\pm$ are defined in eq 4.23. The function $I(u,v)$ can be seen by inspection to be positive, given that $2L \geq d$ (from eq 4.28), implying that ΔU is negative. Any nonplanar membrane configuration (and such a configuration must be adopted by a membrane adhering to a rough substrate) will give an additional bending energy cost in the definition (eq 2.12) and so decrease U.

Equation 4.29 is illustrated in Figure 7. The adhesion energy decreases for larger d as the membrane adopts a more and more nonplanar configuration. For small d/a, one can show that eq 4.29 becomes

$$\frac{\Delta U}{\lambda^2\sigma} = -\frac{a^3\chi^4}{4\xi^2 L}\left(\frac{d}{a}\right)^3 + O\left(\left(\frac{d}{a}\right)^4\right) \quad (4.31)$$

and vanishes as $d \to 0$, in agreement with Figure 7. For larger values of d/a, Figure 7 would seem to imply that ΔU continues to grow in magnitude. This implication, of course, is false and is an unfortunate artifact of going beyond the valid limit of our perturbation theory. Exact numerical solutions for a similar scenario will be discussed in a companion paper[20] and do not exhibit such unphysical behavior.

Again, we emphasize that the parameters specifying the substrate geometry (λ and d in this case) were chosen so that the constraint in eq 4.11 was obeyed.

D. An Isolated Pit. We next consider a single cylindrical pit of radius r and depth λr. Equation 4.4 is now only a function of $\rho = \sqrt{x^2+y^2}$ and is solved by Bessel functions (see Appendix A), as is usual for systems with cylindrical symmetry

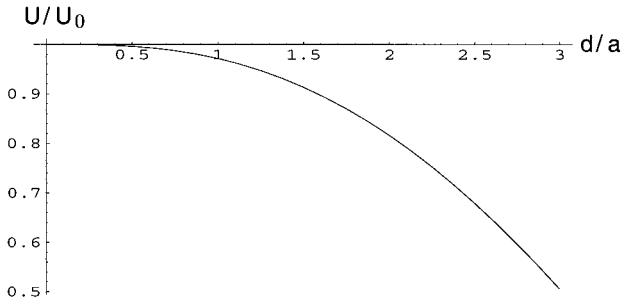

Figure 7. The relative adhesion energy, U/U_0, plotted for a trench of width d and depth λd, with $\lambda = 0.2$. For an isolated, nonplanar perturbation of the substrate, a local definition of the adhesion energy needs to be used and involves the cutoff L (see text). All other parameters used here are given in Table 1 (for strong adhesion case).

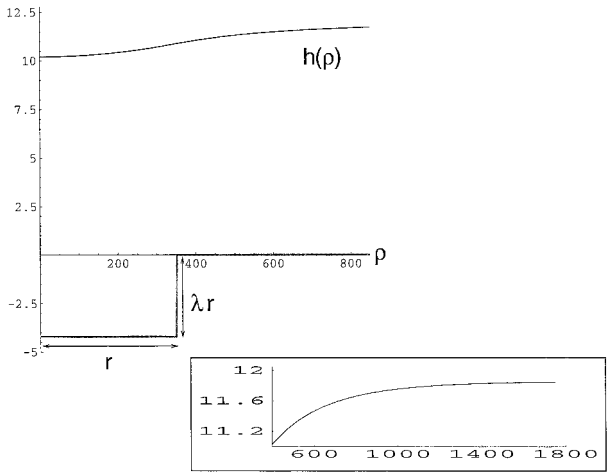

Figure 8. A typical membrane configuration $h(\rho)$ (of the lower lipid leaflet) weakly adhering over a cylindrically symmetric pit of depth λr and radius r, where $\lambda = 0.012$ and $r = 350a \simeq 0.997\ \mu$m (for further choices see Table 1 for weak adhesion). The local adhesion energy (with $L \simeq 259.1a$) is $U/U_0 \simeq 0.50$. The inset shows that no overshoot is present as $\eta_\pm$ are now real. All lengths are given in units of a.

$$\delta h(\rho) = c_0 I_0(\rho\eta_-) + c_1 K_0(\rho\eta_-) + c_2 I_0(\rho\eta_+) + c_3 K_0(\rho\eta_+) + z_s \quad (4.32)$$

Here, $z_s = -\lambda r$ for $\rho < r$ and is zero elsewhere. Requiring a finite solution at $\rho = 0$ and a vanishing one as $\rho \to \infty$, implies that

$$\delta h(\rho) = \begin{cases} c_0 I_0(\rho\eta_-) + c_2 I_0(\rho\eta_+) - \lambda r & \text{for } \rho < r \\ c_1 K_0(\rho\eta_-) + c_3 K_0(\rho\eta_+) & \text{for } \rho > r \end{cases} \quad (4.33)$$

The constants of integration can be found by imposing continuity at $\rho = r$.

The cylindrical symmetry results in little qualitative changes from the previous section (see Figure 8). However, our perturbation theory is now acceptable up to a large hole of radius $r = 350a \simeq 0.997\ \mu$m because of the much smaller nonplanar area of the substrate. A quick glance at Table 1 shows that in this case, $\eta_\pm$ are real, and from eqs A3 and 4.24, no overshoot can then occur.[41] This can also be seen in Figure 8. A local adhesion energy can be defined similarly to eq 4.26, with the cut-off L obeying

(41) Like the exponentials in eq 4.18, $K_0(\eta)$ and $I_0(\eta)$ are single-valued functions for real $\eta > 0$, and so an overshoot can only occur for complex η.

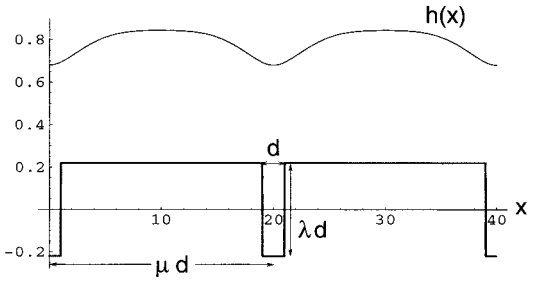

Figure 9. The profile of a membrane $h(x)$ supported (strong adhesion) above a periodically structured substrate with trenches of infinite length, width d, and depth λd. We have set $\lambda = 0.22$, $\mu = 10$, and $d = 2a \simeq 99$ Å in the above. The membrane configuration (thin line) follows that of the substrate (thick line) but at a much reduced amplitude (due to the effects of rigidity and tension). All lengths are shown in units of a.

$$L = 8 \times \max\left(r, \frac{1}{Re\{\eta_+\}}\right) \tag{4.34}$$

Unfortunately, for this case, ΔU is a very complicated expression and it is not possible to proceed analytically. Therefore, as in Section 4C, ΔU is calculated using eq 4.26, with the solution given by eq 4.33 but then the integrals are evaluated numerically. One finds that U decreases with r in a manner similar to that in Figure 7.

E. Periodic Array of Trenches. The next, more complicated scenario to consider is a periodic array of one-dimensional trenches. These trenches are of depth λd and width d in the x direction, and infinitely long in the y direction. We let the length of the repeating unit making up the surface be μd (see Figure 9), then

$$z_s(\rho) = \frac{1}{2}\lambda d - \lambda d \sum_{n=-\infty}^{\infty} [\theta(x - n\mu d + d/2) - \theta(x - n\mu d - d/2)] \tag{4.35}$$

summing over integer n.

By ensuring that the solution is locally symmetric about each trench center, it is possible to write out, using eq 4.18, δh explicitly over one period

$$\delta h(x) = \begin{cases} c_0 \cosh(\eta_+ x) + c_1 \cosh(\eta_- x) - \dfrac{\lambda d}{2} & \text{for } 0 < x < d/2 \\ c_2 e^{\eta_+ x} + c_3 e^{-\eta_+ x} + c_4 e^{\eta_- x} + c_5 e^{-\eta_- x} - \dfrac{\lambda d}{2} & \text{for } d/2 < x < \mu d - d/2 \\ c_0 \cosh(\eta_+(x - \mu d)) + c_1 \cosh(\eta_-(x - \mu d)) - \dfrac{\lambda d}{2} & \text{for } \mu d - d/2 < x < \mu d \end{cases} \tag{4.36}$$

Because the configuration taken up by the membrane is symmetric around $x = \mu d/2$,

$$\delta h(x) = \delta h(\mu d - x) \tag{4.37}$$

one can show that $c_3 = c_2 e^{\eta_+ \mu d}$ and $c_5 = c_4 e^{\eta_- \mu d}$ and so reduce the number of unknowns to four. These unknowns can be found by imposing continuity of δh and its derivatives at $x = d/2$.

The change in adhesion energy (to second-order in δh) is

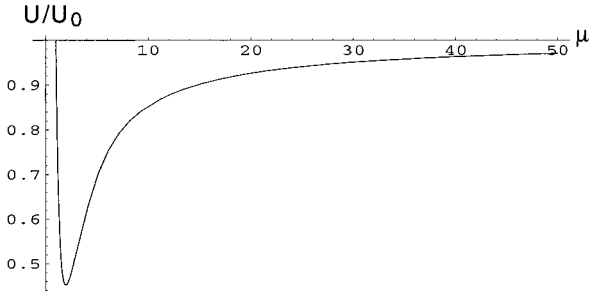

Figure 10. For $\lambda = 0.12$ and $d = 2a \simeq 99$ Å, the relative adhesion energy, U/U_0, in the strong adhesion case is plotted against μ, the periodicity parameter. For the two flat limiting surfaces, $\mu = 1$ and $\mu = \infty$, the decrement ΔU is zero and $U = U_0$. The minimum in the curve occurs near $\mu = 2$, as described in Section 4E.

$$\Delta U = -\frac{1}{\mu d}\int_0^{d/2} dx[\sigma(\delta h')^2 + \kappa(\delta h'')^2 + v(\delta h + \lambda d/2)^2] - \frac{1}{\mu d}\int_{d/2}^{\mu d/2} dx[\sigma(\delta h')^2 + \kappa(\delta h'')^2 + v(\delta h - \lambda d/2)^2] \tag{4.38}$$

and after some algebra, can be found to satisfy

$$\frac{\Delta U}{\sigma} = -\frac{\lambda^2}{2\mu}[I(\Lambda_+,\Lambda_-) + I(\Lambda_-,\Lambda_+)] \tag{4.39}$$

where we define

$$I(u,v) = \frac{(e^u - 1)(e^{(\mu-1)u} - 1)}{e^{\mu u} - 1}\frac{uv^2}{(u^2 - v^2)^2}\left[v^2 - 2\left(\frac{d}{\xi}\right)^2 \chi^4\right] \tag{4.40}$$

recalling that $\Lambda_\pm = \eta_\pm d$. Again, it is possible to show that ΔU is always negative. Note, that the dependence of the adhesion energy on the depth of the trenches, via λ and from eq 4.39, is simply parabolic (providing eq 4.11 holds).

For a surface roughness of this form, an interesting consequence of eq 4.39 is that the excess adhesion energy, ΔU, has a minimum as a function of μ at $\mu = \mu^*$. This phenomenon is illustrated for a strongly adhering membrane in Figure 10. If we use $\epsilon \equiv d/\xi$ as an expansion parameter, (for Figure 10, $\epsilon \simeq 0.11$), then perturbation theory gives

$$\frac{\Delta U}{\lambda^2 \sigma} = -\frac{\mu - 1}{2\mu^2}\chi^4\epsilon^2 + \frac{(\mu - 1)^2}{1440\mu}(\mu^2 + 2\mu - 2)\chi^8\epsilon^6 + O(\epsilon^8) \tag{4.41}$$

Equation 4.41 implies that

$$\mu^* = 2 - \frac{\chi^4}{30}\epsilon^4 + O(\epsilon^6) \tag{4.42}$$

This implication can be understood by looking at the average height of the surface,

$$\langle z_s \rangle = \frac{1}{\mu d}\int_0^{\mu d} dx\, z_s(x) = \frac{\lambda d}{2}\left(1 - \frac{2}{\mu}\right) \tag{4.43}$$

For $1 < \mu < 2$, as μ increases, eq 4.43 evaluated near $\mu = 1$ implies that the surface can be visualized as an array of spikes perturbing an "initial" planar state with $\langle z_s \rangle = -\lambda d/2$. For $\mu = 1$, the substrate is flat and

consequently the general solution, eq 4.18, implies that the membrane is also flat, with $\delta h = -\lambda d/2$ and $U = U_0$. As the thickness of the spikes increases, the membrane responds and is forced to bend more and more. This bending costs energy and ΔU increases in magnitude. However, for $\mu > 2$, the surface (and hence the membrane) starts to tend towards another, "final", planar state of $\langle z_s \rangle = \lambda d/2$, which occurs when $\mu = \infty$. Because δh of the membrane, at this extreme point, also satisfies $\delta h = \lambda d/2$ (i.e., the membrane is flat), $|\Delta U|$ decreases with growing μ. Looking at the two extreme values, $\mu = 1$ and $\mu = \infty$, one can see from eqs 4.39 and 4.40, that ΔU vanishes as expected.

This behavior becomes more transparent if the variance in the height of the surface is considered

$$\langle \Delta z_s^2 \rangle = \langle (z_s - \langle z_s \rangle)^2 \rangle = \left(\frac{\lambda d}{\mu}\right)^2 (\mu - 1) \tag{4.44}$$

with the average defined in eq 4.43. Equation 4.44 vanishes for $\mu = 1$ and $\mu = \infty$, and has a maximum at $\mu = 2$. Therefore, we find that the excess adhesion energy is greatest (in magnitude) for that value of μ at which the surface is the most rough (i.e., $\mu = 2$). In fact, if U is plotted against $\langle \Delta z_s^2 \rangle$, it is just a monotonically decreasing function. From eqs 4.41 and 4.44 we have

$$\frac{\Delta U}{\sigma} = -\frac{\chi^4 \langle \Delta z_s^2 \rangle}{2d^2} \epsilon^2 + O(\epsilon^6) \tag{4.45}$$

and, at this level of approximation, there is a simple, linear relationship.

The average height of the membrane is

$$\langle h \rangle = h_0 + \langle \delta h \rangle = h_0 + \frac{\lambda d}{2}\left(1 - \frac{2}{\mu}\right) \tag{4.46}$$

and $\mu = 2$ again arises as a significant value. It is also interesting to examine the extent to which the membrane penetrates each of the trenches. Concentrating on $\delta h(0)$, we find

$$\frac{\delta h(0)}{\lambda d} = \Lambda_+^2 \Lambda_-^2 \left\{ \frac{I(\Lambda_+) - I(\Lambda_-)}{\Lambda_+^2 - \Lambda_-^2} \right\} - \frac{1}{2} \tag{4.47}$$

where

$$I(u) = -\frac{e^{-u/2}}{u^2} \frac{e^{\mu u} - e^u}{e^{\mu u} - 1} \tag{4.48}$$

and $\Lambda_\pm = \eta_\pm d$. Hence, at the level of the Deryagin approximation, there is a linear dependence on the trench depth, λd. Looking at $h_0 + \delta h(0) - \langle z_s \rangle$, from eq 4.43, one can see [as $I(u)$ is a monotonically increasing function] that the membrane always penetrates further into the trenches as their depth grows. The membrane experiences a more attractive potential due to the greater surface area of the substrate. However, one must be aware that increasing λ can quickly cause eq 4.11 to be broken.

Finally, in Figure 11 we plot $\delta h(0)$ against the periodicity parameter, μ. It is, perhaps, at first sight surprising to see that for large μ, $\delta h(0)$ does not vanish. However, this function is the wrong one with which to take this limit, as one always has at least one trench in the system and is always looking at the depth in this trench. If $\delta h(\mu d/2)$ is considered instead, this parameter tends quite rapidly to $\lambda d/2$, and the membrane returns to its height above a planar substrate. However, one can see from Figure 11 that for $\mu \simeq 8$, the trenches no longer have a significant effect and $\delta h(0)$ plateaus; the membrane effectively experiences a potential generated by a flat surface.

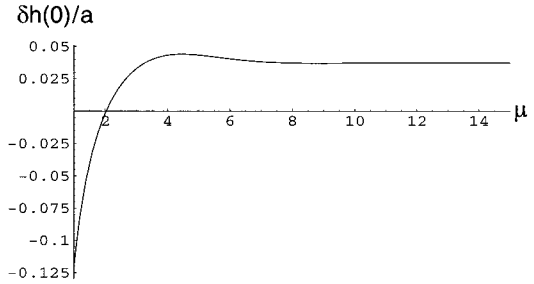

Figure 11. The height deviation of the membrane in the middle of a trench (strong adhesion), $\delta h(0) = h(0) - h_0$, as a function of μ for fixed $\lambda = 0.12$ and $d = 2a \simeq 99$ Å.

F. Tensionless Membranes. So far we have only considered membranes that have a finite tension, σ, and now, for the sake of completeness, we will briefly illustrate how our results change in the limit of $\sigma \to 0$. For vanishing membrane tension, the definitions given in eqs 2.16, A3, and A4 imply that

$$\eta_\pm = \pm \frac{1}{\sqrt{2}}(1 \pm i)\xi_\kappa^{-1} \qquad \text{for } \sigma = 0 \tag{4.49}$$

Equation 4.18 then indicates that the profile will have an oscillatory though exponentially damped form.

To see how U alters, we can look at, for example, the adhesion energy of Section 4E given by eq 4.39, which is valid for a surface periodically patterned with trenches. Multiplying eq 4.39 by σ, one is naturally led to consider

$$\frac{\sigma \chi^4}{\xi^2} \to \kappa \xi_\kappa^{-4} \tag{4.50}$$

in the limit of zero tension. A little thought then gives

$$\Delta U = \frac{\lambda^2}{\mu}\left(\frac{d}{\xi_\kappa}\right)^2 \kappa \xi_\kappa^{-2} [I(\Lambda_+, \Lambda_-) + I(\Lambda_-, \Lambda_+)] \tag{4.51}$$

with

$$I(u, v) = \frac{(e^u - 1)(e^{(\mu-1)u} - 1)}{e^{\mu u} - 1} \frac{uv^2}{(u^2 - v^2)^2} \tag{4.52}$$

and $\Lambda_\pm = d\eta_\pm$, where $\eta_\pm$ are given by eq 4.49. Although it is not as obvious as before, ΔU is again negative.

5. Discussion

In this paper, we have looked at the effect of geometric surface structure on the adhesion properties of a membrane and a solid substrate. The membrane interacts with the substrate via a van der Waals potential and experiences either a Helfrich-like entropic repulsion, if it is weakly adhering, or hydration forces, if it is strongly adhering (supported membrane). We find it convenient to use the Deryagin approximation in which the entire interaction potential is expressed analytically as a local function of membrane height. By making a further harmonic approximation, one can solve for quite a large number of surface geometries.

The nonplanar substrate leads to an interaction potential, which is position dependent, and therefore to the membrane following the surface shape. However, this rough membrane configuration is damped due to the membrane tension and bending rigidity and is unfavorable because of its bending energy cost. Short wavelength undulations are very difficult for the membrane to mimic and two lengthscales, ξ_σ and ξ_κ, analogous to the "healing" length[17] for interfaces in wetting problems, emerge and control the membrane damping.

We find on very general grounds that increasing the roughness of the surface reduces the membrane adhesion energy. Note that the adhesion energy is always calculated per unit of *projected area* to facilitate comparison with the planar surface case. The structured substrate leads to a competition between the bending and potential energy contributions to the free energy; the bending energy tries to flatten the membrane and so move it away from the surface to heights where the effect of the geometrical heterogeneity is strongly reduced. On the other hand, the potential energy is attractive and acts to bring the membrane in closer to the solid surface.

Looking at eq 4.2, we can see that the local Deryagin approximation leads to the surface height entering the free energy only with a term describing the deviation of the membrane away from its planar height. Remembering that we are approximating the interaction potential as a harmonic one (having a parabolic shape), the substrate roughness acts to push the membrane potential energy away from its minimum, V_0. This behavior resembles that of thermal fluctuations. Consequently, the absolute value of the potential energy is reduced relative to the planar case. In addition, the free energy is further increased due to the extra bending energy contribution, which is always absent for flat membrane configurations. This *rise* in the free energy leads to a reduction in the probability that the membrane lies close to the substrate and so to a *decrease* in the adhesion energy.

These considerations are borne out by the particular examples considered in the text. Sinusoidal surfaces, trenches, and pits all act to reduce the membrane adhesion energy U. The rougher the surface, the less likely a membrane is to adhere. This inverse dependence of U is perhaps best illustrated in Figure 10, which refers to surfaces patterned with a regular array of infinitely long trenches. Here, by changing μ, a parameter controlling the distance between successive trenches, we move through different surface configurations whose roughness passes through a maximum. The adhesion energy clearly responds to such behavior, going through a minimum at the point of maximum substrate roughness.

The membrane is unable to "feel" very small scale surface undulations because of the resulting high bending energy cost of adapting to them and the resulting adhesion energy is almost unchanged from its planar value. Figure 3 shows that, for a sinusoidal substrate, U gradually decreases as the surface undulations grow and eventually plateaus at short wavelengths.

As mentioned in Section 1, supported membranes are invaluable for the construction of biosensors.[7−9] The proteins that endow the membrane with these properties can, unfortunately, disturb it from a favorable planar configuration. One way to surmount this problem is to indent the substrate with pockets that then act as "docking" pods for the proteins. However, this technique can be disadvantageous in that the membrane itself may change its configuration significantly in response to the now nonplanar surface. Consequently, we have concentrated on looking at substrates sculptured by trenches and pits.

Our work predicts that the narrower the trench or pocket (Figure 6) and the more widely spaced apart they are (Figure 11), the less likely is the membrane to penetrate into them. Wider trenches are more favorable because the bending energy of the resulting configuration is less. The membrane is flatter in wider trenches and also gains more potential energy because it is able to straighten out at the trench base and lie closer to the surface. We also find that increasing the trench depth (within the limits of our perturbation theory) encourages membrane penetration into them.

The membrane can also overshoot (similar to the behavior in a laser trap[31]) near a disturbance in the planar structure of the surface. Overshooting (i.e., having a height greater than that it would have had for a completely flat surface) occurs for $2\xi > \xi_\sigma$ (at least, within Deryagin) and consequently is directly due to the membrane having a finite (non-zero) rigidity.

To summarize, a membrane is less likely to adher to a rough substrate. It tries to follow the substrate surface but only does so for long wavelength fluctuations because of their low bending energy cost. Thus, the membrane prefers to enter broad, widely separated indentations.

In an accompanying paper,[20] we will explore nonlocal methods, which enable progress beyond the Deryagin approximation, and also will perform some exact numerical calculations. We shall extend the method to include chemical heterogeneity, which then opens up the possibility of modeling chemically and geometrically structured substrates that are becoming crucial to new, pioneering biotechnological research.

Acknowledgment. We are particularly grateful to J. Rädler and E. Sackmann for introducing us to the problem of membrane adhesion on rough surfaces, for numerous discussions and suggestions, and for sharing with us their experimental results. We greatly benefited from conservations and correspondence with M. Kozlov, A. Marmur, P. Lenz, R. R. Netz, M. O. Robbins, U. Seifert, and P. B. Sunil Kumar. P.S.S. would like to thank the British Council, the Israeli Ministry of Science, and the Sackler Institute for Theoretical Physics (Tel Aviv University) for providing financial support during a visit to Israel, where the majority of this work was carried out. Partial support from the Israel Science Foundation founded by the Israel Academy of Sciences and Humanities-Centers of Excellence Program is gratefully acknowledged.

Appendix A: Solution of the Euler−Lagrange Equation for Piecewise Constant Surfaces

In some cases, and in particular if z_s is piecewise continuous, it is more convenient to work directly in real space (as opposed to Fourier space). To find the membrane profile, one must then solve eq 4.4 and use eq 4.2 to calculate U. Given a piecewise constant surface, eq 4.4 becomes

$$(\kappa\nabla^4 - \sigma\nabla^2 + v)(\delta h(\boldsymbol{\rho}) - z_s) = 0 \qquad \text{(A1)}$$

for a constant z_s (but which changes value discontinuously for different ranges of $\boldsymbol{\rho}$).

The operator in eq A1 can be factorized

$$\kappa\nabla^4 - \sigma\nabla^2 + v = \kappa(\nabla^2 - \eta_+^2)(\nabla^2 - \eta_-^2) \qquad \text{(A2)}$$

where $\eta_\pm$ are complex in general and satisfy

$$\eta_\pm = \xi^{-1}\left[\frac{1 \pm \sqrt{1 - 4\chi^4}}{2}\right]^{1/2} \tag{A3}$$

with

$$\chi = (\kappa v/\sigma^2)^{1/4} = \frac{\xi}{\xi_\kappa} \tag{A4}$$

a dimensionless ratio of lengths. For our chosen set of parameters (Table 1), $\chi \simeq 0.302$ and $\chi \simeq 9.44$ for weak and strong adhesion, respectively.

Therefore, to solve eq A1, which is a fourth-order differential equation, we can consider equivalently two coupled second-order differential equations,

$$(\nabla^2 - \eta_-^2)(\delta h(\boldsymbol{\rho}) - z_s) = u_0(\boldsymbol{\rho}) \tag{A5}$$

$$(\nabla^2 - \eta_+^2)u_0(\boldsymbol{\rho}) = 0 \tag{A6}$$

for the function $\delta h(\rho)$ and a second function $u_0(\rho)$. However, because of the underlying linearity of the second-order differential equations, the general solution is simply

$$\delta h(\boldsymbol{\rho}) = c_0 u_0(\boldsymbol{\rho}) + c_1 u_1(\boldsymbol{\rho}) + z_s \tag{A7}$$

with constants c_0, c_1, and z_s, and where $u_1(\boldsymbol{\rho})$ satisfies

$$(\nabla^2 - \eta_-^2)u_1(\boldsymbol{\rho}) = 0 \tag{A8}$$

Thus, we have reduced the fourth-order differential equation to two familiar second-order Helmholtz equations. This approach is most useful for systems with cylindrical or spherical symmetry.

Appendix B: Kink Configurations in Membranes and Interfaces

In this Appendix, we consider the elastic energy cost of a membrane adopting a configuration containing sharp kinks. Let us, for the purpose of illustration, consider a one-dimensional membrane embedded in a two-dimensional space having the profile

$$h(x) = c\,\tanh\left(\frac{x}{\epsilon L}\right) \tag{B1}$$

with the two lengths L and c obeying $L \gg c$. In the limit of $\epsilon \to 0$, $h(x)$ develops two sharp kinks

$$\lim_{\epsilon \to 0} h(x) = c[2\theta(x) - 1] \tag{B2}$$

and becomes a step function. We can examine the effect this has on the asymptotic behaviors of the two adhesion energy densities (per unit area)

$$u_\sigma = \frac{\sigma}{2L}\int_{-L}^{L} dx\,\sqrt{1 + h'^2} \tag{B3}$$

and

$$u_\kappa = \frac{\kappa}{2L}\int_{-L}^{L} dx\,\frac{h''^2}{(1 + h'^2)^{5/2}} \tag{B4}$$

Equations B3 and B4 provide the contributions to the free energy from the tension (interface-like) and the rigidity (membrane-like) terms in eq 2.2, respectively.

The interfacial elastic energy cost is simply proportional to the length of the membrane in the step configuration

$$u_\sigma \simeq \frac{\sigma}{2L}2(L + c)$$

$$\sim \sigma \tag{B5}$$

where we have taken the limit of $\epsilon \to 0$. This is clearly finite.

To find the asymptotic limit of the rigidity contribution, we notice that

$$u_\kappa = \frac{2c^2\epsilon\kappa}{L^5}\int_{-L}^{L} dx\,\frac{\tanh^2\left(\frac{x}{\epsilon L}\right)\cosh^{-4}\left(\frac{x}{\epsilon L}\right)}{\left[\epsilon^2 + \left(\frac{c}{L}\right)^2\cosh^{-4}\left(\frac{x}{\epsilon L}\right)\right]^{5/2}} \tag{B6}$$

is an even function and so, writing $t = \tanh(x/\epsilon L)$, we have

$$u_\kappa = \frac{4c^2\kappa}{\epsilon^3 L^4}\int_0^{\tanh(1/\epsilon)} dt\,\frac{t^2(1 - t^2)}{\left[1 + \left(\frac{c}{\epsilon L}\right)^2(1 - t^2)^2\right]^{5/2}} \tag{B7}$$

which can be integrated by parts

$$u_\kappa \sim \frac{2\kappa}{3L^2\epsilon}\left\{1 - \int_0^{\tanh(1/\epsilon)} \frac{dt}{\left[1 + \left(\frac{c}{L}\right)^2\left(\frac{1 - t^2}{\epsilon}\right)^2\right]^{3/2}}\right\} \tag{B8}$$

Because

$$\lim_{\epsilon \to 0}\left\{\frac{1 - \tanh^2(1/\epsilon)}{\epsilon}\right\} = 0 \tag{B9}$$

the integral in eq B8 is well-defined and finite.

Therefore, for small ϵ, we have

$$u_\sigma \sim \sigma \quad \text{and} \quad u_\kappa \sim \frac{\kappa}{L^2}\epsilon^{-1} \tag{B10}$$

and so the tension or interface-like contribution is constant, whereas that from the rigidity (membrane-like) diverges. Therefore, an interface ($\kappa = 0$ and $\sigma \neq 0$) can have a configuration with a sharp kink, whereas a membrane cannot.

LA990503M